Nonsaturating linear resistivity up to 900 K in MgB_2

I. Pallecchi,[1] C. Belfortini,[2] F. Canepa,[2] C. Ferdeghini,[1] P. Manfrinetti,[2] A. Palenzona,[2] R. Vaglio,[3] and M. Putti[1]
[1]*CNR-INFM-LAMIA and Università di Genova, via Dodecaneso 33, 16146 Genova, Italy*
[2]*DCCI, CNR-IMEM Unità di Genova and Università di Genova, via Dodecaneso 31, 16146 Genova, Italy*
[3]*CNR-COHERENTIA and Università di Napoli "Federico II," Complesso di Monte S. Angelo, Via Cinthia, 80126 Napoli, Italy*
(Received 13 January 2009; published 8 April 2009)

In this work, we report resistivity measurements on MgB_2 polycrystalline samples with increasing degree of doping (disorder) up to temperatures higher than 900 K. In all cases the normal state curves are linear with increasing temperatures, with no sign of flattening or downward bending (saturation) at high temperature. This behavior, in sharp contrast to what is observed in superconducting compounds such as A15 and Chevrel phases, can be explained considering the dominant π contribution to the electric conduction, together with the smaller electron-phonon coupling of π carriers in MgB_2, as compared to characteristic coupling strength of those compounds. This indicates that in MgB_2 the disorder introduced in the lattice by thermal oscillations even at 900 K can still be considered as a perturbation within the Boltzmann description of transport.

DOI: 10.1103/PhysRevB.79.134508 PACS number(s): 74.70.Ad, 74.25.Kc, 74.25.Fy

I. INTRODUCTION

Superconductivity in MgB_2 is universally recognized to be of conventional phonon mediated character.[1] In single band superconductors, the transition temperature T_c can be expressed in terms of the electron-phonon coupling constant λ. In turn, λ is closely related to its transport counterpart λ_{tr} (Ref. 2), which determines the temperature dependence of the normal state resistivity.

In the case of a multiband superconductor the situation is more complex and T_c can be expressed in terms of a combination of all the elements of the matrix of the coupling constant coefficients.[3] In MgB_2, the σ and π bands are both coupled with phonons, particularly with the optical E_{2g} mode, but with different intensities: the σ bands are strongly coupled, whereas the π bands are weakly coupled. The two-band model predicts therefore that the high T_c value in MgB_2 is mainly determined by the largest eigenvalue of the coupling matrix, that is, by the coupling coefficient of the σ bands.[3] On the other hand, transport properties are generally dominated by the more conducting bands, less coupled with phonons, namely, the π bands.[4] However, this picture might fail in disordered samples.[4–6] Therefore, the analysis of normal state transport with increasing disorder up to high temperatures is important to explore the role of the two kinds of bands in the different disorder and temperature regimes, which, in turn, is crucial to determine relevant superconducting properties such as the upper critical field.

In most metals, the temperature-dependent resistivity is well described by the generalized Bloch-Grüneisen (B-G) law:

$$\rho(T) = \rho_0 + (n-1)\rho' \Theta_D \left(\frac{T}{\Theta_D}\right)^n \int_0^{\Theta_D/T} \frac{x^n}{(e^x-1)(1-e^{-x})} dx, \tag{1}$$

where ρ_0 is the low-temperature residual resistivity due to impurity scattering, Θ_D is the Debye temperature, ρ' is the coefficient of the high-temperature linear slope and n is a coefficient between 3 and 5. According to the Bloch-Grüneisen theory, the temperature dependence at all but the lowest temperatures arises from the assumption that the scattering cross section for electrons is largely proportional to the mean square thermal motion of the atoms, linearly proportional to T at high temperatures. Yet, in many "conventional" superconducting compounds, a downward curvature and a corresponding flattening of the resistivity curve, which is commonly referred to as "saturation," are observed at high temperature. For example, such anomalous saturation is observed in A15 compounds such as V_3Si, Nb_3Pt, Nb_3Al (Ref. 7), Nb_3Sn (Ref. 8), Nb_3Ge, V_3Ge (Ref. 9), Chevrel phases,[10] transition-metal alloys,[11] and iron oxypnictides.[12] On the other hand, no saturation is observed in ZrN (Ref. 13) and other compounds[14–16] as well as in high-T_c and other nonconventional superconductors, despite in most cases the resistivity reaching values even larger than those of A15 and other saturating compounds.

The most crude explanation of resistivity saturation is that, when the charge carrier mean free path ℓ approaches the interatomic spacing a, the classical Boltzmann theory breaks down and the concept of mean free path itself loses validity, because the uncertainty in the **k** vector of an electron is comparable to the size of the Brillouin zone. The resistivity reaches its saturation value ρ_{sat} when $\ell \sim a$, which is known as the Ioffe-Regel criterion.[17] Wiesmann *et al.*[18] first introduced the phenomenological parallel resistor model:

$$\frac{1}{\rho(T)} = \frac{1}{\rho_{ideal}(T)} + \frac{1}{\rho_{sat}}, \quad \text{with } \rho_{sat} \approx \frac{v_F}{\varepsilon_0 \Omega_p^2 a}, \tag{2}$$

where v_F is the Fermi velocity, Ω_p is the plasma frequency, ρ_{ideal} is described by the Bloch-Grüneisen law and the residual resistivity becomes $\rho(0) = (\frac{1}{\rho_0} + \frac{1}{\rho_{sat}})^{-1}$. Experimental values of ρ_{sat} fall between 100 and 300 $\mu\Omega$ cm in most of the above-mentioned superconductors.

This simple parallel resistor approach fails in explaining why the resistivities of ZrN and other compounds do not saturate, and, in many cases, either overestimates or underestimates the experimental ρ_{sat} value.[19–21] Alternative explanations of the resistivity saturation have been proposed in-

 ©2009 The American Physical Society

TABLE I. Parameters of Al-doped samples $Mg_{1-x}Al_xB_2$: Al content x, transition temperature, defined at 90% of the normal state resistivity value, transition width, defined as the temperature interval where resistivity drops from 90% to 10% of its normal state value, residual resistivity evaluated at 40 K, resistivity difference $\Delta\rho=\rho(300\ \mathrm{K})-\rho(40\ \mathrm{K})$, rescaled residual resistivity calculated as $\rho(40\ \mathrm{K})\cdot(7.5\ \mu\Omega\ \mathrm{cm})/\Delta\rho$ (see text) and residual resistivity ratios RRR, defined as $\rho(300\ \mathrm{K})/\rho(40\ \mathrm{K})$.

$Mg_{1-x}Al_xB_2$ sample name	Al content x	T_c (K)	ΔT_c (K)	$\rho(40\ \mathrm{K})$ ($\mu\Omega$ cm)	$\Delta\rho$ ($\mu\Omega$ cm)	Rescaled $\rho(40\ \mathrm{K})$ ($\mu\Omega$ cm)	RRR
S0	0	39.2	0.2	0.61	9	0.51	15
S1	0.15	33.4	0.4	13.5	12	8.30	1.9
S2	0.3	27.3	6.0	14.1	8	13.3	1.6
S3	0.4	25.1	17.0	23.2	9	19.4	1.4

cluding thermal smearing in superconducting compounds characterized by sharp structures in the density of states near the Fermi level,[22] unusual phonon anharmonicity,[23] phonon mode softening,[24] and thermal expansion of the lattice.[25] More recently Millis[16] proposed a model based on the breakdown of Migdal approximation for large electron-lattice coupling that well accounts for most experimental observations.

All these possible mechanisms were extensively reviewed by Gunnarsson *et al.*[26] The same authors[26,27] introduced a new approach, and calculated the resistivity behavior in the limit of very strong scattering, linking the latter to the behavior of the optical conductivity $\sigma(\omega)$. In their treatment, the Ioffe-Regel criterion is derived quantum mechanically and many cases of violation of such criterion are explained. Generally, the Ioffe-Regel criterion for resistivity saturation is fulfilled in large bandwidth noninteracting systems. A simple formula, derived for d electrons in transition metal compounds, is given by Gunnarsson, Calandra, and Han to evaluate the saturation resistivity:

$$\rho_{\mathrm{sat}} = C\frac{V}{a^3}\frac{\hbar a}{N_d e^2}, \tag{3}$$

where $C\approx 5$ is a dimensionless factor that depends on the details of the electronic structure, V is the volume of the unit cell, and e is the electron charge.

The aim of the present paper is to report on measurements up to high temperatures (900 K) on MgB_2 samples with different disorder levels and to discuss the results within the two-band picture. Our purpose is to detect any anomaly in the resistivity curves, by approaching on the one hand the limit of validity of the Boltzmann theory $\ell \sim a$ and on the other hand the breakdown of the Migdal approximation for large electron-lattice coupling. The former regime is achieved by increasing both disorder (decreasing ℓ due to impurity scattering) and temperature (decreasing ℓ due to phonon scattering), while the latter regime is achieved by increasing temperature (increasing electron-lattice interaction). The case of MgB_2 is of particular interest, because in order to observe any possible transport crossover between bands, a broad temperature range must be spanned, but, to the best of our knowledge, the only measurements of MgB_2 samples at high temperature carried out up to now reach 400 K (Ref. 28) and 450 K.[29] Moreover, a further reason for exploring a large temperature range is due to the higher Debye temperature of MgB_2 compared to most superconducting compounds, including A15s.[30]

II. EXPERIMENTAL RESULTS AND DISCUSSION

In order to explore the MgB_2 resistivity curves also as a function of disorder, a series of $Mg_{1-x}Al_xB_2$ samples (called here S0-S3) was prepared by the technique described elsewhere.[31] Irradiated samples[32] are not suitable for this purpose because defects are recovered by annealing at relatively low temperatures.[33] The morphology of the samples studied by scanning electron microscope analyses shows that the undoped sample is formed by hexagonal shaped grains of about 2–5 μm in size, while the Al-doped ones consist of smaller and irregularly shaped grains (<1 μm), with less porosity.[34]

The transition temperatures T_c of our Al-doped samples (defined at 90% of the normal state resistivity value) monotonically decrease from 39.2 K to 25.1 K and the residual resistivity values $\rho(40\ \mathrm{K})$ monotonically increase with increasing doping, for substitutions up to 40%, as reported in Table I.

Four probe resistivity measurements are carried out from room temperature down to 5 K in a PPMS Quantum Design commercial system and from room temperature up to almost 1000 K in a homemade apparatus. In this equipment, the electrical contacts are realized by copper leads mechanically pressed on the sample by springs and the temperature is measured by a chromel-alumel thermocouple. The heating rate is about 0.5 K/min in order to minimize the stress due to the different thermal expansion coefficients of the sample holder components. A vacuum of nearly 10^{-5} mbar is maintained throughout each measurement.

We focus our study on the resistivity curve shape, without exploring how the absolute value of resistivity evolves with disorder, since ρ in MgB_2 is dramatically affected by the sample connectivity.[35] This has been taken into account by Rowell[35] rescaling the data in such a way that $\Delta\rho=\rho(300\ \mathrm{K})-\rho(40\ \mathrm{K})$ is forced to be a fixed value. In Table I, we report the values of $\Delta\rho$, which, in our case, do not vary very much from sample to sample, but without following any monotonic trend. We rescale the resistivity curves by keeping $\Delta\rho\sim 7.5$ $\mu\Omega$ cm for all samples, which is chosen as an av-

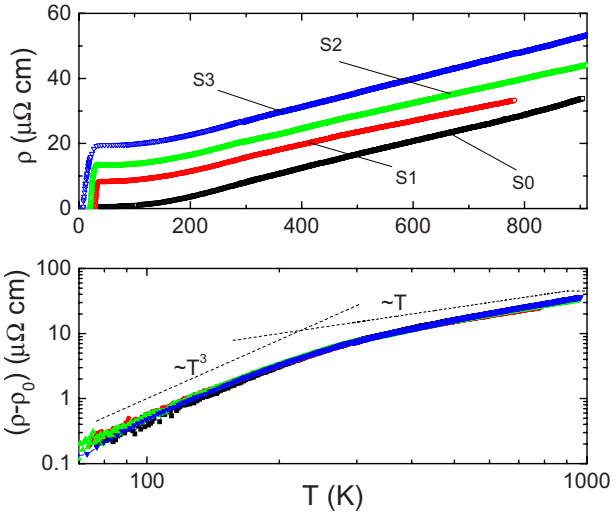

FIG. 1. (Color online) Upper panel: Rescaled resistivity curves of Al-doped samples up to 910 K. Lower panel: same resistivity curves, after subtraction of the respective residual resistivity values, plotted in log-log scale. The dashed lines indicate T^3 and T slopes.

erage among experimental $\Delta\rho$ values found in literature.[36] The rescaled residual resistivity values of our Al-doped samples, which range from 0.51 $\mu\Omega$ cm to 19.4 $\mu\Omega$ cm, are reported in Table I. We point out that the scaling procedure clearly hides small changes in $\Delta\rho$ due to intrinsic reasons. However it has been suggested that material parameters such as electron-phonon coupling, plasma frequency, and density of states are not strongly affected by low level Al substitutions.[37]

In the upper panel of Fig. 1, we show the rescaled experimental resistivity curves up to 910 K. It can be seen at a glance that all the curves follow an overall linear trend at high temperatures. Weak but detectable superlinear and sublinear deviations from linearity are observed that could be related Mg loss as demonstrated by a thin layer of conducting Mg found on the walls of the sample chamber after each measurement. Despite irreversible Mg loss, no phase transformation takes place during heating, as demonstrated by x-ray analysis; indeed, MgB_2 decomposition is expected to occur around 1130 K at 10^{-5} mbar (Ref. 38), beyond the range of our measurements. We also notice that the abrupt jump at 450 K observed by Shen[29] is not present in our data, as it is related to oxidation of free Mg at the grain boundaries, not occurring in our measurements, which are carried out in vacuum.

In the lower panel of Fig. 1, we plot the same resistivity curves in a log-log scale, subtracting the respective residual resistivity values. Such plot emphasizes that all the curves collapse, presenting the same T^3 behavior at low temperatures and linear T behavior at high temperature. We conclude that no crossover of transport between σ and π bands does occur.[4] This proves that at all temperatures the resistivity is dominated by the π band (the one less coupled with phonons) only, even in the most doped samples. Such outcome, not obvious *a priori*, especially in the temperature range where impurity scattering is not negligible, due to the Al doping introduced disorder in the π band,[39] justifies the application of the Rowell criterion to disordered samples in a self-consistent way.

TABLE II. Parameters ρ' obtained by fitting resistivity curves of Al-doped samples up to 900 K by using the Bloch-Grüneisen law (1) and the corresponding transport electron-phonon coupling constant λ_{tr} calculated by Eq. (4).

Sample	ρ' ($\mu\Omega$ cm K^{-1}) B-G fit	λ_{tr}
S0	3.8×10^{-2}	0.36
S1	3.6×10^{-2}	0.38
S2	3.7×10^{-2}	0.40
S3	3.9×10^{-2}	0.45

The most important outcome evident from Fig. 1, for our purposes, is the high-temperature linear behavior, which indicates no resistivity saturation. Indeed, the four resistivity curves are well described by the generalized Bloch-Grüneisen Eq. (1), with $n=3$, the same value of Θ_D around 1035 K and values of the temperature coefficient ρ' ranging from 0.036 to 0.039 $\mu\Omega$ cm K^{-1}. The coefficient $n=3$ is expected in multiband systems, where the conduction in one band prevails and this band is strictly correlated with the others by interband scattering processes.[40] This situation fairly applies to MgB_2: indeed, in the regime of phonon scattering the inter- and intraband scattering rates of the π carrier are comparable, yet remaining always much smaller than the intraband scattering rate of the σ carriers.[4]

For the sake of simplicity, and supported by the above observation that at all temperatures the resistivity is dominated by the π band, we are neglecting here the two-band transport.[41] In Table II the ρ' fitting values are reported, together with the transport electron-phonon coupling constants λ_{tr}, which are approximately extracted from ρ' using the single band relation:

$$\lambda_{tr} \approx \frac{\hbar\varepsilon_0\Omega_p^2}{2\pi K_B}\rho', \tag{4}$$

where Ω_p is the plasma frequency of the relevant band averaged over the crystallographic directions ($\Omega_{p\pi}$ values for the pure sample and for different Al contents are taken from Refs. 42 and 43 and listed in Table III), $\hbar$ is the Planck constant, ε_0 the vacuum dielectric constant, and K_B the Boltzmann constant. We point out, however, that the extracted λ_{tr} absolute values must be taken with some caution, as they clearly depend on the value imposed to $\Delta\rho$. Our extracted $\lambda_{tr(\pi)}$ values (Table II) well agree with theoretical evaluations by Monni and co-workers[44] that give $\lambda_{tr(\pi)}\approx0.43$ and $\lambda_{tr(\sigma)}\approx0.93$. Al doping is suggested to decrease severely λ_σ, while density of states of π band increases with doping, suggesting an increased λ_π,[37,43] as experimentally observed. Furthermore, we notice that the transport coupling constant values given in Table II are pretty small as compared to typical coupling constants of other superconducting compounds that exhibit high-temperature resistivity saturation (e.g., $\lambda\sim1.7$ for Nb_3Sn, $\lambda\sim1.7-1.9$ for Nb_3Ge, $\lambda\sim1.4-1.6$ for Nb_3Al). Instead, they are comparable with coupling constants of non-

TABLE III. Theoretical parameters for Al-doped samples, taken form Ref. 43, namely, plasma frequencies and Fermi velocities of the π and σ bands, averaged over the crystalline directions. In the last three columns, values of saturation resistivities calculated either from the Ioffe-Regel criterion Eq. (2) considering the π band only (sixth column), or from the Ioffe-Regel criterion Eq. (2) considering the π and σ bands in parallel (seventh column), or from the Gunnarsson-Calandra model Eq. (3) (last column). In the latter case, there is no dependence on Al content, since we neglect the few percent variation in the lattice parameters.

Sample	$\Omega_{p\pi}$ (Hz)	$\Omega_{p\sigma}$ (Hz)	$v_{F(\pi)}$ (m/s)	$v_{F(\sigma)}$ (m/s)	ρ_{sat} from Eq. (2) with π band parameters ($\mu\Omega$ cm)	ρ_{sat} from Eq. (2) with π and σ bands in parallel ($\mu\Omega$ cm)	ρ_{sat} from Eq. (3) ($\mu\Omega$ cm)
S0	9.32×10^{15}	5.04×10^{15}	5.78×10^{5}	3.28×10^{5}	423	279	474
S1	9.79×10^{15}	4.38×10^{15}	6.21×10^{5}	3.01×10^{5}	412	291	474
S2	1.01×10^{16}	3.44×10^{15}	6.76×10^{5}	2.60×10^{5}	423	325	474
S3	1.03×10^{16}	2.78×10^{15}	7.26×10^{5}	2.60×10^{5}	435	362	474

saturating superconducting compounds such as ZrN ($\lambda \sim 0.6$) (Ref. 13).

We can now estimate the value of ρ_{sat} for MgB_2 using the simple Ioffe-Regel Eq. (2). The Fermi velocities as a function of Al content can be calculated as $v_{F(\pi,\sigma)i}=\frac{\Omega_{p(\pi,\sigma)i}}{q}\sqrt{\frac{\varepsilon_0}{N_{(\pi,\sigma)}}}$ (Table III), using the values of the density of states N_π and N_σ and plasma frequencies calculated in Ref. 43. In this equation, the subscript i indicates the crystallographic direction. Assuming the boron-boron distance $a\approx1.780\times10^{-10}$ m as lattice spacing, neglecting the variations of lattice parameters due to Al doping and considering the π band only, we obtain the ρ_{sat} values listed in Table III, around ~423 $\mu\Omega$ cm for the different Al doping levels, all well above the largest measured resistivity $\rho(900\ \mathrm{K})\approx53$ $\mu\Omega$ cm of our most doped sample. If we considered the σ and π bands in parallel, we would obtain smaller ρ_{sat} values from 280 to 360 $\mu\Omega$ cm for the four samples, as also reported in Table III. For the electron-phonon scattering mean free path, we have[19]

$$\ell \approx \frac{\hbar v_F}{2\pi\lambda_{tr}K_BT}G(T)$$

$$\text{where}\quad G(T)=2\left(\frac{T}{\Theta_D}\right)^3\int_0^{\Theta_D/T}\frac{x^3}{(e^x-1)(1-e^{-x})}dx, \tag{5}$$

which gives, at 900 K, $\ell\approx1.5-1.9$ nm with π band parameters, 1 order of magnitude larger than the lattice spacing a. If we considered the σ and π bands in parallel, the ℓ values would turn out to be smaller, not far from the lattice spacing value.

We can estimate the expected saturation resistivity value also using the Gunnarsson relation (3). In MgB_2, four orbitals contribute to transport: the $\pi1$ and $\pi2$ bands, formed by the p_z orbitals of boron atoms, and the $\sigma1$ and $\sigma2$ bands, formed by sp^2-hybridized orbitals stretched along boron-boron bonds; thereby, this yields $N_d=4$ in Eq. (3). Assuming $a\approx1.780\times10^{-10}$ as above, we obtain $\rho_{sat}\approx474$ $\mu\Omega$ cm.

In Fig. 2 we report the experimental curves for S0 and S3 samples, as representative of the whole set of samples. The latter sample should be the best of the series to look for saturation effects, since it presents the largest resistivity, but with increasing Al doping the plasma frequencies increase and the Fermi velocities change in such a way that saturation resistivities increase. Smaller saturation resistivity values are indeed expected for the undoped sample S0 (see Table III). For each sample, two theoretical fitting curves, also plotted in the figure, are obtained using the parallel resistor formula with ρ_{ideal} given by the Bloch-Grüneisen Eq. (1) and two different ρ_{sat} values, namely, the largest and the smallest of those reported in Table III. The largest ρ_{sat} is the Gunnarsson-Calandra saturation resistivity from Eq. (3)

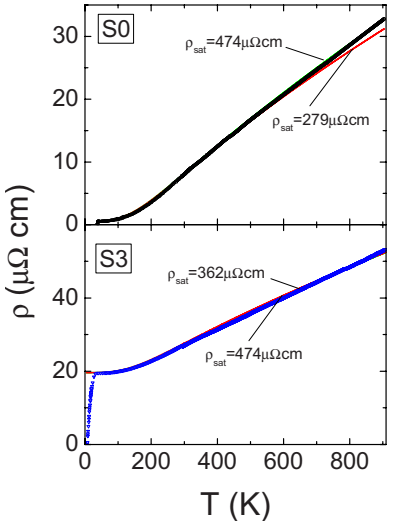

FIG. 2. (Color online) Rescaled resistivity curves of the undoped MgB_2 sample S0 (upper panel) and most doped $Mg_{0.6}Al_{0.4}B_2$ sample S3 (lower panel) together with the fitting curves obtained (i) with ρ_{ideal} given by the B-G Eq. (1) and ρ_{sat} obtained from the Gunnarsson-Calandra Eq. (3), assuming four intermixed bands (green continuous lines, not distinguishable from experimental data points in this scale, in both panels) and (ii) with ρ_{ideal} given again by the B-G Eq. (1) and ρ_{sat} obtained from Ioffe-Regel formula (2) assuming π and σ bands in parallel (red dashed lines, clearly distinguishable from experimental data points at the highest temperatures in the upper panel).

(ρ_{sat}=474 $\mu\Omega$ cm for both S0 and S3 samples); the smallest one is the Ioffe-Regel saturation resistivity with the two bands π and σ in parallel (ρ_{sat}=279 $\mu\Omega$ cm for S0 and ρ_{sat}=362 $\mu\Omega$ cm for S3). It is clear that for sample S3 all our estimations of ρ_{sat} using either Ioffe-Regel or Calandra-Gunnarsson relations nearly overlap with experimental data. However, for the S0 sample, a departure from linearity at the highest temperatures would be expected in the hypothesis of the Ioffe-Regel formula with two bands in parallel (ρ_{sat} =279 $\mu\Omega$ cm), while no sign of such departure is seen in the experimental data. Instead, the Gunnarsson-Calandra saturation resistivity well describes the experimental curve of S0. These results show that the parallel conduction between σ and π bands fails to account for the resistivity versus temperature behavior; indeed, the distinction between σ and π bands is meaningless in the frame of high phonon scattering and short mean free path. On the other hand, provided that only the π band is taken into account, the simple Ioffe-Regel equation explains the absence of saturation in MgB_2 up to 900 K. This indicates that such effects as temperature-dependent bandwidth and temperature-dependent hopping kinetic energy play no role in large bandwidth MgB_2. Similarly, also the Gunnarsson criterion describes the absence of saturation, taking into account all the four π and σ bands.

As already explained, we cannot inspect the evolution of $\Delta\rho$ with disorder in our experiment; however, such analysis is possible on Gandikota's experimental data on 2 MeV alpha particles disordered MgB_2 films.[45] In that case, due to their specific irradiation technique, carried out on the same sample in successive steps, $\Delta\rho$ should not be affected by changes in intergrain connectivity. They found that $\Delta\rho$ decreases by 30% as the residual resistivity increases and they ascribe it to resistivity saturation. However we calculate that ascribing this decrease to saturation effects would lead to ρ_{sat}=407 $\mu\Omega$ cm, only slightly smaller than the Gunnarsson-Calandra saturation resistivity. We conclude that the $\Delta\rho$ decrease observed in that experiment may be explained in terms of saturation, but other effects such as DOS decrease cannot be completely ruled out as well.[8]

III. CONCLUSIONS

We report measurements of resistivity curves of MgB_2 polycrystalline samples with increasing degrees of disorder obtained by Al doping. Experimental data available up to temperatures larger than 900 K, never reached before in literature to the best of our knowledge, provide information on transport mechanisms in MgB_2.

The temperature-dependent terms of all the samples merge together and present a T^3 behavior at low temperatures and linear T behavior at high temperature. This allows to achieve two main conclusions: (1) in the whole temperature range no crossover of transport between σ and π bands does occur with increasing disorder and only the most conducting channel is effective (π). (2) No flattening out of the resistivity curves is detected even in the most resistive samples, which instead are well described by the Bloch-Grüneisen law.

The absence of saturation in our experimental data indicates that in MgB_2 the disorder induced in the periodic lattice by thermal vibrations and doping is not dramatic enough to cause the breakdown of the Boltzmann description, so that electron-phonon coupling can be treated perturbatively, even at temperatures as large as 900 K.[16] In this respect, the crucial parameter is the coupling constant of the π band electrons ($\lambda_{tr(\pi)} \approx 0.4$), which is low in comparison with values of most superconducting compounds ($\lambda_{tr(\pi)} > 1$).

ACKNOWLEDGMENTS

The authors would like to acknowledge M. Calandra and J. M. Rowell for helpful discussion. They also acknowledge financial support from the Italian Foreign Affairs Ministry (MAE)—General Direction for the Cultural Promotion.

[1] J. M. An and W. E. Pickett, Phys. Rev. Lett. **86**, 4366 (2001).
[2] B. Chakraborty, W. E. Pickett, and P. B. Allen, Phys. Rev. B **14**, 3227 (1976); P. B. Allen, T. P. Beaulac, F. S. Khan, W. H. Butler, F. J. Pinski, and J. C. Swihart, *ibid.* **34**, 4331 (1986).
[3] I. I. Mazin and V. P. Antropov, Physica C **385**, 49 (2003).
[4] I. I. Mazin, O. K. Andersen, O. Jepsen, O. V. Dolgov, J. Kortus, A. A. Golubov, A. B. Kuz'menko, and D. van der Marel, Phys. Rev. Lett. **89**, 107002 (2002).
[5] M. Putti, R. Vaglio, and J. M. Rowell, Supercond. Sci. Technol. **21**, 043001 (2008).
[6] M. Ortolani, D. Di Castro, P. Postorino, I. Pallecchi, M. Monni, M. Putti, and P. Dore, Phys. Rev. B **71**, 172508 (2005).
[7] R. Caton and R. Viswanathan, Phys. Rev. B **25**, 179 (1982).
[8] Z. Fisk and G. W. Webb, Phys. Rev. Lett. **36**, 1084 (1976).
[9] L. R. Testardi, J. M. Poate, and H. J. Levinstein, Phys. Rev. B **15**, 2570 (1977).
[10] C. S. Sunandana, J. Phys. C **12**, L165 (1979).
[11] J. H. Mooij, Phys. Status Solidi A **17**, 521 (1973).
[12] D. Bhoi, P. Mandal, and P. Choudhury, Supercond. Sci. Technol. **21**, 125021 (2008).
[13] A. Cassinese, M. Iavarone, R. Vaglio, M. Grimsditch, and S. Uran, Phys. Rev. B **62**, 13915 (2000).
[14] A. F. Hebard, T. T. M. Palstra, R. C. Haddon, and R. M. Fleming, Phys. Rev. B **48**, 9945 (1993).
[15] A. W. Tyler, A. P. Mackenzie, S. NishiZaki, and Y. Maeno, Phys. Rev. B **58**, R10107 (1998).
[16] A. J. Millis, J. Hu, and S. Das Sarma, Phys. Rev. Lett. **82**, 2354 (1999).
[17] A. F. Ioffe and A. R. Regel, Prog. Semicond. **4**, 237 (1960).
[18] H. Wiesmann, M. Gurvitch, H. Lutz, A. Ghosh, B. Schwarz, M. Strongin, P. B. Allen, and J. W. Halley, Phys. Rev. Lett. **38**, 782 (1977).
[19] F. Nava, O. Bisi, and K. N. Tu, Phys. Rev. B **34**, 6143 (1986).
[20] H. Takagi, B. Batlogg, H. L. Kao, J. Kwo, R. J. Cava, J. J. Krajewski, and W. F. Peck, Jr., Phys. Rev. Lett. **69**, 2975 (1992).
[21] N. L. Wang, C. Geibel, and F. Steglich, Physica C **262**, 231

(1996).
[22] R. W. Cohen, G. D. Cody, and J. J. Halloran, Phys. Rev. Lett. **19**, 840 (1967).
[23] M. Gurvitch, Physica B&C **135**, 276 (1985).
[24] L. R. Testardi and T. B. Bateman, Phys. Rev. **154**, 402 (1967).
[25] B. Sundqvist and B. M. Andersson, Solid State Commun. **76**, 1019 (1990).
[26] O. Gunnarsson, M. Calandra, and J. E. Han, Rev. Mod. Phys. **75**, 1085 (2003).
[27] M. Calandra and O. Gunnarsson, Phys. Rev. Lett. **87**, 266601 (2001).
[28] T. Masui, K. Yoshida, S. Lee, A. Yamamoto, and S. Tajima, Phys. Rev. B **65**, 214513 (2002).
[29] J. Q. Shen, M. H. Fang, Y. Zheng, H. T. Wang, Y. Lu, and Z. A. Xu, Physica C **386**, 663 (2003).
[30] B. Cort, G. R. Stewart, C. L. Snead, A. R. Sweedler, and S. Moehlecke, Phys. Rev. B **24**, 3794 (1981); R. Viswanathan and R. Caton, *ibid.* **18**, 15 (1978).
[31] M. Putti, C. Ferdeghini, M. Monni, I. Pallecchi, C. Tarantini, P. Manfrinetti, A. Palenzona, D. Daghero, R. S. Gonnelli, and V. A. Stepanov, Phys. Rev. B **71**, 144505 (2005).
[32] C. Tarantini, H. U. Aebersold, V. Braccini, G. Celentano, C. Ferdeghini, V. Ferrando, U. Gambardella, F. Gatti, E. Lehmann, P. Manfrinetti, D. Marré, A. Palenzona, I. Pallecchi, I. Sheikin, A. S. Siri, and M. Putti, Phys. Rev. B **73**, 134518 (2006).
[33] R. H. T. Wilke, S. L. Bud'ko, P. C. Canfield, J. Farmer, and S. T. Hannahs, Phys. Rev. B **73**, 134512 (2006).
[34] I. Pallecchi, V. Braccini, E. G. d'Agliano, M. Monni, A. S. Siri, P. Manfrinetti, A. Palenzona, and M. Putti, Phys. Rev. B **71**, 104519 (2005).
[35] J. M. Rowell, Supercond. Sci. Technol. **16**, R17 (2003).
[36] M. Eisterer, Supercond. Sci. Technol. **20**, R47 (2007).
[37] A. Bussmann-Holder and A. Bianconi, Phys. Rev. B **67**, 132509 (2003).
[38] S. Brutti, A. Ciccioli, G. Balducci, G. Gigli, P. Manfrinetti, and A. Palenzona, Appl. Phys. Lett. **80**, 2892 (2002).
[39] M. Putti, C. Ferdeghini, M. Monni, I. Pallecchi, C. Tarantini, P. Manfrinetti, A. Palenzona, D. Daghero, R. S. Gonnelli, and V. A. Stepanov, Phys. Rev. B **71**, 144505 (2005).
[40] G. T. Meaden, *Electrical Resistance of Metals* (Heywood Books, London, 1966), p. 89.
[41] Two-band transport would require two expressions of the form of Eq. (1) in parallel. In this case, the residual resistivities of each band would not be unambiguously determined by the measured residual resistivity, so that the fitting procedure would not have univocal results. In any case we estimate that the high-temperature linear derivative approaches the π band value within 10%, depending on how the residual resistivity is shared between π and σ bands.
[42] A. Brinkman, A. A. Golubov, H. Rogalla, O. V. Dolgov, J. Kortus, Y. Kong, O. Jepsen, and O. K. Andersen, Phys. Rev. B **65**, 180517(R) (2002).
[43] G. Profeta, A. Continenza, and S. Massidda, Phys. Rev. B **68**, 144508 (2003).
[44] M. Monni, I. Pallecchi, C. Ferdeghini, V. Ferrando, A. Floris, E. Galleani d'Agliano, E. Lehmann, I. Sheikin, C. Tarantini, X. X. Xi, S. Massidda, and M. Putti, Europhys. Lett. **81**, 67006 (2008).
[45] R. Gandikota, R. K. Singh, J. Kim, B. Wilkens, N. Newman, J. M. Rowell, A. V. Pogrebnyakov, X. X. Xi, J. M. Redwing, S. Y. Xu, and Q. Li, Appl. Phys. Lett. **86**, 012508 (2005).